Building and Environment 160 (2019) 106191

Contents lists available at ScienceDirect

Building and Environment

journal homepage: www.elsevier.com/locate/buildenv

# Reduced-scale experiments on the thermal performance of phase change material wallboard in different climate conditions

Yuhao Qiao[a,b], Liu Yang[a,b], Jiayang Bao[a,b], Yan Liu[a,b,*], Jiaping Liu[a,b]

[a] State Key Laboratory of Green Building in Western China, Xi'an University of Architecture and Technology, Xi'an, Shaanxi, 710055, PR China
[b] School of Architecture, Xi'an University of Architecture and Technology, Xi'an, Shaanxi, 710055, PR China

ARTICLE INFO

*Keywords:*
Artificially controlled condition
Climate characteristics
Phase change material
Reduced-scale experiments
Thermal performance

ABSTRACT

Integrating phase change material (PCM) into building envelope is an effective approach for establishing a comfortable indoor thermal environment in the summer. The full exploitation of thermal storage performance of PCM envelope depends on the suitability of the outdoor climate conditions. There is one key question should be solved: How to quantitatively describe the effects of local climate characteristics on the thermal storage performance of PCM envelope? Thus, in the present study, the thermal storage performance of PCM wallboard is investigated under different climate conditions in reduced-scale experiments with artificially controlled conditions. The typical meteorological year in 10 cities in Northern and Western China are determined to extract the experimental conditions. Based on the degree hours concept, evaluation indices are developed to quantitatively analyze the climate characteristics, including the accumulative temperature during a whole day and the accumulated temperature difference between the outdoor air temperature and phase change temperature. The combined effect of the range of variation in the temperature and the accumulated temperature are obtained base on the indices. Reductions in the accumulated temperature of over 88% are observed under the climate conditions in Xi'an and Kashi. However, the reduction is only 36.8% under the condition in Xining. Finally, with nonlinear regression analysis. The relationship between the thermal storage effect of PCM wallboard and the accumulated temperature difference is determined by nonlinear regression analysis. The results provide a reference to assess the suitability and appropriate thermal design for PCM envelope in different climate conditions.

## 1. Introduction

A stable indoor thermal environment is beneficial for establishing a comfortable living space [1]. Due to the continental climate in China, the temperature daily ranges are generally large, especially in Northern and Western China, with hot days and cool nights in the summer [2]. Therefore, improving the thermal performance of the building envelope in these areas is important for stabilizing indoor thermal environment [3]. Fluctuations in the indoor temperature can be effectively suppressed by enhancing the thermal storage performance of the building envelope [4]. A suitable indoor thermal environment is achieved in traditional dwellings by employing heavy structures, such as the Yaodong dwellings on the Loess Plateau [5], Ayiwang style in Xinjiang [6], and earth buildings in dry–hot climate areas [7]. However, due to the development of urbanization, the conventional methods are no longer considered suitable because a large amount of thermal mass would be required to increase the thermal inertia of urban buildings [8]. Therefore, it is imperative to identify suitable thermal storage materials for integration in the envelope of modern building that occupy less of the effective building space [9]. Previous studies suggest that phase change material (PCM) is useful thermal storage material for buildings because of their excellent thermal physical properties, which allow them to store and release large amounts of latent heat during the phase change process within a specific temperature range [10]. Therefore, the integration of PCM in building envelope is a promising approach for improving the indoor thermal environment in buildings.

Two main issues have been investigated in previous PCM envelope research. The first is the effect of applying PCM envelope. These studies mainly focused on the effects on the indoor thermal environment, reducing the heating/cooling energy consumption by using PCM envelope, and the thermal performance of PCM envelope under local climate conditions. Recently, many experimental studies were conducted under actual climate conditions to directly determine the effect of PCM envelope. In particular, Lee et al. [11] built two test houses

* Corresponding author. State Key Laboratory of Green Building in Western China, Xi'an University of Architecture and Technology, Xi'an, Shaanxi, 710055, PR China.
*E-mail address:* liuyan@xauat.edu.cn (Y. Liu).

https://doi.org/10.1016/j.buildenv.2019.106191
Received 7 April 2019; Received in revised form 16 May 2019; Accepted 6 June 2019
Available online 07 June 2019
0360-1323/ 

**Nomenclature**

| | |
|---|---|
| $c$ | specific heat capacity, kJ·kg$^{-1}$·ºC$^{-1}$ |
| $E$ | accumulated difference between the outdoor air temperature and phase change temperature over 24 h, ºC·h |
| $I$ | degree hours based on the average hourly temperature, ºC·h |
| $I_L$ | intensity of long-wave radiation from a thermally black body at outdoor air temperature, W·m$^{-2}$ |
| $I_T$ | intensity of direct plus diffuse solar radiation on the outer surface of the wall, W·m$^{-2}$ |
| $P$ | temperature attenuation ratio, % |
| $Q$ | thermal storage capacity, J |
| $q$ | heat flux, W·m$^{-2}$ |
| $q_{ex,\ sur}$ | heat flux on the exterior surface of the PCM wallboard, W·m$^{-2}$ |
| $q_{in,\ sur}$ | heat flux on the interior surface of the PCM wallboard, W·m$^{-2}$ |
| $R$ | thermal resistance of the external surface/air interface, m$^2$·ºC·W$^{-1}$ |
| $T$ | temperature, ºC |
| $T_{air}$ | dry-bulb temperature of outdoor air, ºC |
| $T_{ave}$ | average hourly temperature in a day, ºC |
| $T_e$ | outdoor air temperature, ºC |
| $T_{ex,\ air}$ | outdoor air temperature of the test cell, ºC |
| $T_{ex,\ sur}$ | exterior surface temperature of the PCM wallboard, ºC |
| $T_i$ | hourly temperature in each hour of the whole day ($i$ = 1, 2, 3 … 24), ºC |
| $T_{in,\ air}$ | indoor air temperature of the test cell, ºC |
| $T_{in,\ sur}$ | interior surface temperature of the PCM wallboard, ºC |
| $T_{max}$ | maximum hourly temperature, ºC |
| $T_{min}$ | minimum hourly temperature, ºC |
| $T_{PC}$ | phase change temperature, ºC |
| $T_R$ | daily temperature range, ºC |
| $T_{sa}$ | sol-air temperature, ºC |

*Greek letters*

| | |
|---|---|
| $\alpha$ | absorptivity for solar radiation, dimensionless |
| $\Delta H$ | latent heat of PCM, kJ·kg$^{-1}$ |
| $\Delta T$ | temperature fluctuation range on interior surface, ºC |
| $\varepsilon$ | emissivity for infrared radiation of the considered wall, dimensionless |
| $\lambda$ | thermal conductivity, W·m$^{-1}$·ºC$^{-1}$ |
| $\rho$ | density of materials, kg·m$^{-3}$ |

*Abbreviations*

| | |
|---|---|
| CSWD | Chinese Standard Weather Data |
| EPS | extruded polystyrene |
| PCM | phase change material |
| PVC | polyvinyl chloride |
| TSVL | thermal storage and ventilation laboratory |

located in Kansas (the U.S. DOE Region 4) to evaluate the reduction effect of peak heat flux using PCM envelope. The PCM was combined with insulation material and placed in the walls at the north, east, south, and west of the test cells. They found that the hourly average peak heat flux was reduced by 20.1%. In addition, Akeiber et al. [12] developed a kind of PCM that was extracted from crude petroleum waste product for application in hot climate conditions. The roofs and walls integrated with PCM exhibited excellent energy saving performance by reducing the heat flux and temperature fluctuations. PCM was also been applied to demonstration buildings, such as in the Fraunhofer ISE project in Germany [13], where a lightweight wall integrated with PCM plaster was combined with night ventilation and shading in a full-size office room, and it effectively adjusted the indoor air temperature. Mourid et al. [14] determined the thermal behavior of a PCM wallboard in a real scale building in Casablanca, Morocco. The heating energy consumption was reduced by 20% in a room with PCM envelope. Barzin et al. [15] adopted PCM-impregnated gypsum boards in two comparative test chambers to reduce the cooling energy utilized in New Zealand during the summer, and the electricity saving was 73% electricity in one week when integrated with night ventilation. PCM have also been combined with intermittent heating equipment and solar energy in winter, and to stabilize temperature fluctuations during the summer in hot regions [16–18]. Lin et al. [17] combined shape-stabilized PCM plates with under-floor electric heating in Beijing, which charged with heat during the night using cheap electricity and discharged the stored heat during the daytime. Kim et al. [18] investigated the effect of PCM on the heating load in Japan during the winter. The shape-stabilized PCM was arranged on the interior surfaces of walls with different areas and thicknesses. Thus, these previous studies mainly focused on the effects of applying PCM envelope to reduce the fluctuations in the indoor air temperature, as well as the energy saving performance when combined with active heating systems and air conditioning systems.

The second key issue is related to the thermal design parameters for the thermal design of PCM envelope. In generally, previous studies of this issue were conducted under artificially controlled conditions in order to quantitatively obtain the influence of different parameters. Recent investigations mainly focused on the thermal performance of PCM wallboards in different ideal conditions including various outdoor air temperature ranges and cycles (such as periodic temperature fluctuations, linear temperature increasing and declines) [19], solar radiation at different intensities [20], and ventilation at various air temperatures and velocities [21]. The thermal design parameters of PCM envelope have also been investigated numerically in controlled conditions, such as the latent heat and thermal conductivity of PCM [22], location of PCM layers [23] and the phase change temperature [24]. Kuznik et al. [25,26] conducted full-scale tests in an artificial climate chamber, where the outdoor air temperature and solar radiation were dynamically simulated. The indoor air temperature was analyzed to evaluate the effect of building envelope with and without applying PCM. The experimental data obtained from these studies have been employed widely to validate numerical models. Sun et al. [27] proposed a pipe-encapsulated PCM for use in building walls and an experimental device called a “dynamic wall simulator” was constructed to obtain indoor and outdoor conditions according to set curves. The design parameters were investigated for PCM pipes in the wall, including different pipe sizes and installation depths. The effects of ventilation and solar radiation on PCM wallboard were determined by Xie et al. [20,28]. The phase change period and heat flux were compared as the ventilation temperature increased from 34 °C to 40 °C and the airflow rate increased from 1 m·s$^{-1}$ to 2.5 m·s$^{-1}$. Moreover, various PCM envelopes with different applications were investigated in terms of their thermal performance under dynamically controlled experimental conditions, such as PCM-filled glass [29], PCM combined with solaria [30], and PCM cooling ceilings [31].

Based on above literature investigations, previous experimental studies of PCM envelope can be classified into two main categories comprising those conducted under actual climate conditions to assess applications and those performed under artificially controlled conditions in order to determine their effects on the thermal performance of PCM envelope. However, it is difficult to quantitatively study the design parameters for PCM envelope under outdoor conditions because the

actual climate is not controlled. Moreover, the experiments conducted under controlled conditions always assume idealized environmental conditions, thereby neglecting the actual variable characteristics of the climate. Therefore, quantitatively describing the relationships between climate characteristics and the thermal storage performance of PCM envelope is a key issue that needs be solved to facilitate the application of PCM envelope in different climates. Based on a previous investigation of thermal design parameters of lightweight PCM wallboard by Yang et al. [32,33], the present work is conducted in an artificial climate chamber with the typical climate conditions found in Northern and Western China. Ten representative cities are selected and the dry-bulb temperatures in July are extracted from typical meteorological year as the experimental controlled conditions. Based on degree hours concept, two indices are developed to describe the climate characteristics in terms of both the temperature range and duration. Moreover, the relationships between the indices and the temperature attenuation ratio are obtained by nonlinear regression analysis. The results obtained in the present study can provide references to facilitate the quantitative analysis the relationships between climate characteristics and the thermal performance of PCM envelope.

## 2. Experimental setup

### 2.1. Properties of the PCM and the experimental wallboard

To choose suitable PCM for building thermal storage, comfortable indoor air temperature is a significant factor. According to the previous research by Yan et al., in Northern and Western China with dry-hot

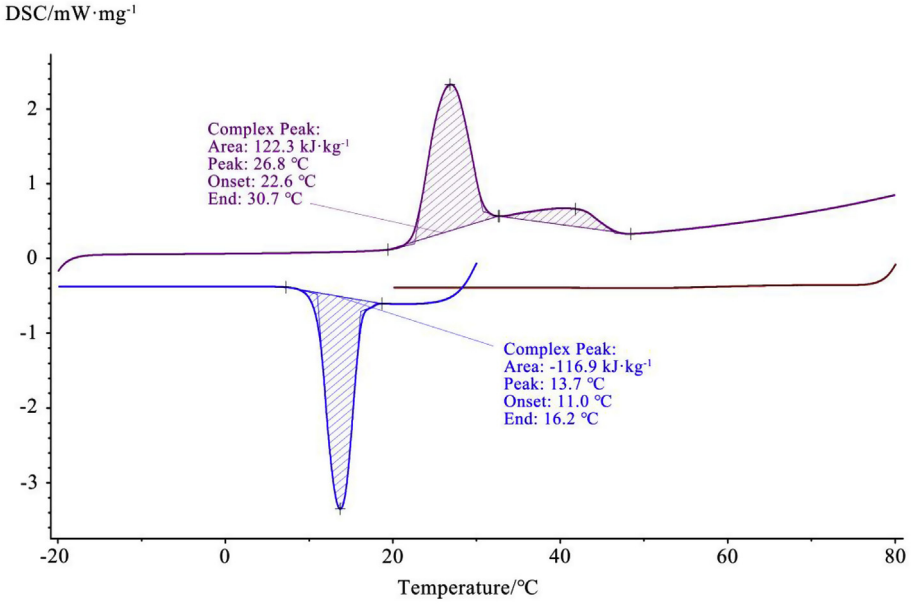


**Fig. 1.** (a) DSC curves of $CaCl_2 \cdot 6H_2O$ [32]; (b) Diagram of PCM with different phase and the encapsulated PCM panel.

climate, the preferred comfortable temperature is 26.5 °C [34]. Therefore, as the thermal mass to adjust indoor air temperature, the PCM should have a phase change temperature closing to the comfort temperature. The PCM with 26 °C phase change temperature is a reasonable choice. On the other hand, the thermal storage and night ventilation technology is a suitability passive cooling technology in the summer of Northern and Western China [6]. The PCM should be conducive to the further application of this technology. According to the outdoor air temperature conditions of Western and Northern China, the PCM with 26 °C phase change temperature has the potential to match the outdoor air temperature and store cold energy from the night ventilation. In addition, due to the reason of appropriate phase change temperature, economy and nonflammable, salt hydrates (such as $CaCl_2{\cdot}6H_2O$) is adopted widely in engineering application and research of building thermal storage [35,36]. Therefore, $CaCl_2{\cdot}6H_2O$ with around 26 °C phase change temperature is adopted as the base material of the macro-encapsulated PCM for the present experiment.

The $CaCl_2{\cdot}6H_2O$ is a kind of inorganic salt hydrates with high latent heat and a low cost. According to the previous study in Ref. [32], the DSC curves of $CaCl_2{\cdot}6H_2O$ are shown in Fig. 1 (a). The DSC test is conducted from −20 °C to 80 °C with 5 °C·min$^{-1}$ temperature change rate. It can be seen from the DSC curves that the melting temperature range is from 22.6 °C to 30.7 °C. The latent heat of $CaCl_2{\cdot}6H_2O$ is 122.3 kJ·kg$^{-1}$ during the melting process and 116.9 kJ·kg$^{-1}$ during the solidification process. In addition, the nucleating agent is mixed into the encapsulated PCM for reducing the supercooling phenomenon of pure $CaCl_2{\cdot}6H_2O$. To avoid leakage by the PCM, it is encapsulated into a polyvinyl chloride (PVC) container. The length, width, and thickness of the PVC container are 520 mm, 220 mm and 20 mm, respectively. The PCM in different phase and encapsulated PCM panel are illustrated in Fig. 1 (b).

As described in the previous study [32], a PCM wallboard comprising macro-encapsulated PCM panels and EPS panels are used. The thickness of the PCM wallboard is 50 mm, with a 20 mm PCM layer and 30 mm EPS layer. The physical parameters of the wallboard materials are listed in Table 1.

### 2.2. Experimental conditions

The Thermal Storage and Ventilation Laboratory (TSVL) experimental system is employed to simulate the actual climate conditions. The system is composed of a climate chamber, controlled system, and a reduced-scale building model called the Thermal Storage and Ventilation test cell (see Fig. 2). The length, width and height in the climate chamber are 4.2 m, 2.7 m and 2.4 m, respectively. The temperature and humidity are simulated by the climate chamber according to set curves. The envelope of the climate chamber comprises 300 mm extruded polystyrene (EPS) and polished aluminum plates. According to the set curves, the air temperature in the climate chamber could be adjusted from 10 °C to 45 °C and the relative humidity from 10% to 90%. The rate of change in the air temperature in the climate chamber is up to 1.2 °C·min$^{-1}$. A test cell with replaceable walls is installed in the climate chamber as a reduced-scale building device. The internal length, width, and height of the test cell are 1.2 m, 0.6 m and 0.8 m. Adiabatic wallboards with 100 mm EPS panels are applied as the envelope of the test cell. One of the adiabatic wallboards is replaced by a PCM wallboard. As shown in Fig. 2, thermocouples and heat flux meters are arranged on the surfaces of the PCM wallboard and the wallboards are tightly sealed. There is no inner heat source in the test cell. The experiments are conducted in the climate chamber with the temperature changes that can be found in Section 3.1. The temperature of the air and the PCM wallboard is carefully recorded by the measurement devices mentioned in Section 2.3. In order to avoid the influence of the initial conditions, each experimental setup is run for 96 h, and the recorded data of the last 48 h is selected as the analysis object.

### 2.3. Measurement devices

Fig. 2 shows the layout of measurement points in the experiments. The surface temperature of the PCM wallboard and interior/exterior air temperature in the test cell are measured using K-type thermocouples. The temperatures are recorded with HOBO® four-channel thermometers. The temperature measurement range for K-type thermocouples is from −200 °C to 1300 °C with a relative error of ± 5%. Heat flux meters are arranged on the interior/exterior surfaces of the PCM wallboard. The heat flux data are recorded using Keithley® data acquisition. The heat flux in the direction from the exterior side to the interior side is defined as a positive value. The output signal is converted by the coefficient of 23.26 W·m$^{-2}$·mV$^{-1}$ to obtain the heat flux value. The temperature and heat flux recording intervals are both 1 min. The sensor Measurement parameters are listed in Table 2.

## 3. Analysis of climate characteristics

### 3.1. Typical climate conditions in northern and western China

The climate conditions considered in the present work comprise hourly outdoor dry bulb temperatures extracted from typical meteorological year of representative cities in Northern and Western China, i.e., Beijing, Xi'an, Xining, Yinchuan, Lanzhou, Urumqi, Hohhot, Dunhuang, Kashi, and Turpan. Wuhan in central China is treated as a reference (see Fig. 3). In the experiments, the average hourly temperature in July for each representative city is applied as a set curve. To representing the dry-bulb temperature characteristics of July, the average hourly dry-bulb temperature of each day in July is obtaining. The steps for obtaining the typical day of the experiment are as follows: First, the hourly dry-bulb temperature of each day on July is obtained from Chinese Standard Weather Data (CSWD). Then, the dry-bulb temperatures of each hour in each day of July is averaged (For example, the dry-bulb temperatures of 8 o'clock in each day of July are averaged). And the average dry-bulb temperatures of 24 h are combined as the set curves of experimentally controlled temperature.

Fig. 4 shows the set curves of experimentally controlled temperature for Xi'an, Lanzhou, Urumqi, and Turpan as examples to illustrate the different local climate conditions. Experimental controlled temperature curves are employed to represent the summer dry-bulb temperature features of the representative cities. In generally, the climate in Northern and Western China is characterized by large daily range of air temperature, which is typical dry hot climate in the summer. Therefore, it is meaningful to increase the thermal inertia of buildings to improve the indoor thermal environment.

**Table 1**
Physical parameters of PCM wallboard materials.

| Materials | ρ/kg·m$^{-3}$ | λ/W·m$^{-1}$·°C$^{-1}$ | c/kJ·kg$^{-1}$·°C$^{-1}$ | ΔH/kJ·kg$^{-1}$ |
|---|---|---|---|---|
| Insulation material | 30 | 0.0376 | 1.2 | – |
| Polyvinyl chloride | 1400 | 0.16 | 0.9 | – |
| Phase change material | 1100 | 1.08 (in solid phase)/0.54 (in liquid phase) | 1.34 (in solid phase)/2.31 (in liquid phase) | 122.3 (melting)/116.9 (solidification) |

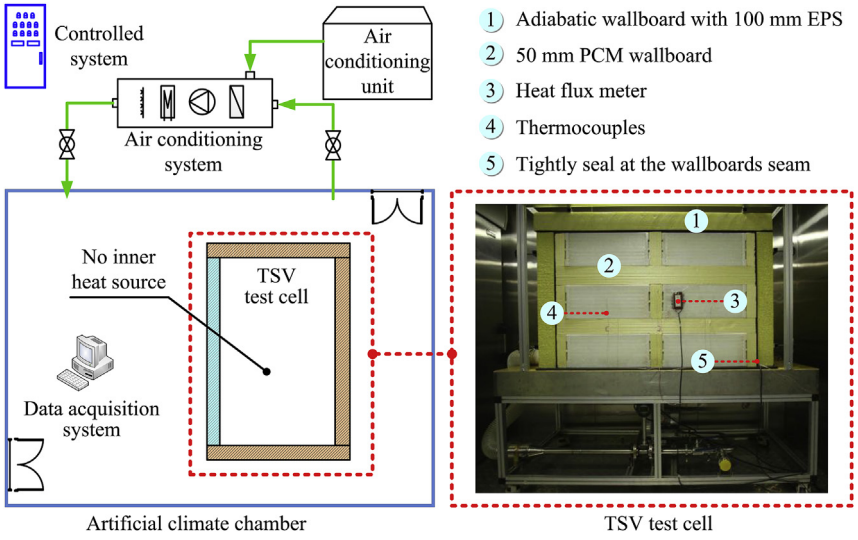


**Fig. 2.** The schematic diagram of experimental system.

**Table 2**
Sensors and their accuracy.

| Sensor | Measurement range | Relative error |
|---|---|---|
| K-type thermocouple | −200-1300 °C | ± 0.5 °C |
| Heat flow meter | −500-500 W·m$^{-2}$ | ≤5% |

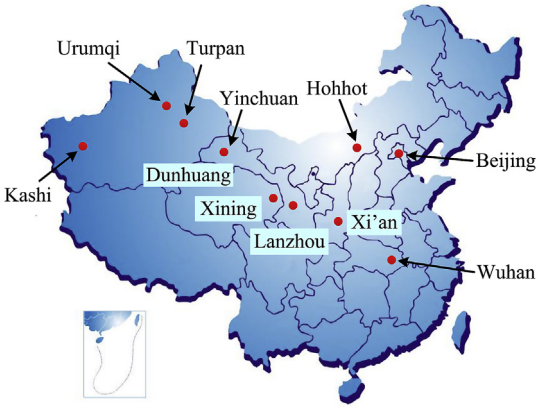


**Fig. 3.** Representative cities in Northern and Western China.

### 3.2. Establishment of climate characteristic indices

The main indices used in previous studies include the daily temperature range, maximum/minimum temperature, and average temperature, which mainly represent aspects of the temperature range [37]. In fact, the duration of the temperature is important in addition to the outdoor air temperature range for thermal storage applications in buildings. Therefore, based on the degree hours concept, two new indices are developed to represent the outdoor air temperature characteristics in the present study. The degree hours based on the average hourly temperature is defined as the index *I*. *E* is the accumulated difference between the outdoor air temperature and the phase change temperature over 24 h. The derived indices are described as follows:

$T_R$ is the daily temperature range and it is calculated as follows:

$$T_R = T_{max} - T_{min} \quad (1)$$

where $T_{max}$ is the maximum hourly temperature; $T_{min}$ is the minimum hourly temperature. $T_{ave}$ is defined as the average hourly temperature in a day:

$$T_{ave} = \frac{\sum_{i=1}^{24} T_i}{24} \quad (2)$$

where $T_i$ is the hourly temperature during a day ($i$ = 1, 2, 3 … 24).

In some cases, the maximum/minimum and average temperature cannot fully reflect the changing characteristics in temperature. For instance, with the same maximum/minimum temperature, the high/low temperature duration may be large and the duration could be small. Thus, the cumulative effect of the outdoor air temperature would be totally different. Therefore, a new index is required. $I$ represents the degree hours based on the average hourly temperature over 24 h and it is expressed as follows:

$$I = \int_0^{24} |T - T_{ave}| dt \quad (3)$$

where $T$ is the temperature of the outdoor air and wall surfaces; $t$ is the time. In contrast to the traditional climate analysis indices, $I$ can represent the cumulative effect of fluctuations in temperature over a period.

The relationships between climate characteristics and the effect of applying of PCM envelope are quantitatively evaluated in this study. The phase change temperature is one of the key design parameters that affect the application of PCM envelope. The thermal storage and release process are significantly influenced by the difference between the phase change temperature and the outdoor air temperature [38]. Therefore, the phase change temperature is adopted to calculate the accumulated difference index ($E$), which is expressed as follows:

$$E = \int_0^{24} (T - T_{PC}) dt \quad (4)$$

where $T_{PC}$ is the phase change temperature. Thus, the outdoor climate characteristics and the thermal storage effect of the PCM wallboard under different climate conditions are obtained based on the indexes ($T_R$, $T_{ave}$, $I$, and $E$).

### 3.3. Analysis of climate characteristics in representative cites

The climate characteristics of the representative cities are analyzed with the indices described in Section 3.2. Fig. 5 (a) illustrates the $T_{max}$ and $T_{min}$ values for each city. In July, the largest $T_{ave}$ is observed in Turpan with 32.8 °C. The lowest $T_{ave}$ occurs in Xining with 17.6 °C. The average $T_R$ in the representative cities is 24.9 °C. The fluctuations in the outdoor air temperature in Turpan reflects the typical continental dry hot climate characteristics, where $T_{max}$ = 39.2 °C and $T_{min}$ = 25.9 °C. Xining has a typical continental climate with large daily temperature

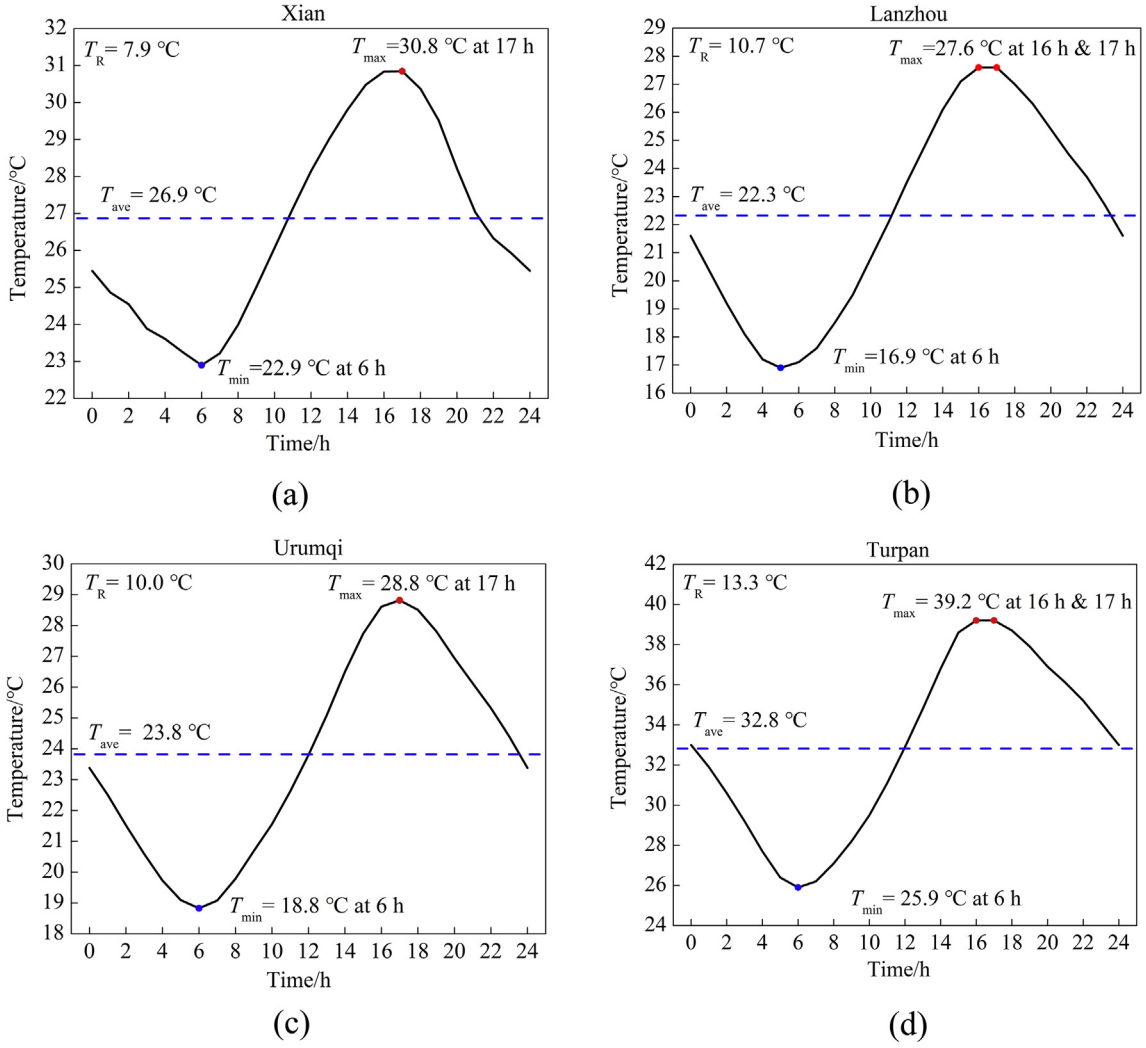


**Fig. 4.** Experimental conditions with representative cities: (a) Xi'an; (b) Lanzhou; (c) Urumqi; (d) Turpan.

range, but the $T_{max}$ value determined as 24 °C indicates that cooling is not a necessary requirement in Xining during the summer. Fig. 5 (b) shows the daily temperature ranges in the representative cities. The average daily temperature range is 10.7 °C, thereby demonstrating the high fluctuations in temperature during the summer in Northern and Western China. Therefore, applying a building envelope with an adequate thermal storage capacity is important in these regions. The outdoor dry bulb temperatures in Dunhuang and Turpan indicated that, $T_R$ is higher than 13.0 °C. However, the temperature in Turpan ranged from 25.9 °C to 39.2 °C, which is far higher than that in the other representative cities. Dunhuang, Kashi, Lanzhou, Yinchuan, Urumqi, and Hohhot in Northern and Western China are characterized by a typical dry hot climate in summer, where $T_R$ is higher than 9 °C and $T_{ave}$ is about 24.9 °C. However, although the average outdoor air temperature in Wuhan is similar to that in other representative cities, the daily temperature range is small at 5.7 °C. Therefore, there is less need to improve the thermal storage performance of buildings in Wuhan compared with other cities. In the early stage of building design, $T_R$ and $T_{ave}$ can be utilized to analyze the climate characteristics. $T_R$ can be employed to evaluate the requirement for using thermal storage technology in different climate conditions. However, $T_R$ and $T_{ave}$ can only represent the climate conditions applied to the PCM envelope. Therefore, the suitability of PCM envelope cannot be fully reflected by $T_R$ and $T_{ave}$.

The indices described above, including $I$ and $E$, could more accurately depict the characteristic temperature changes in terms of the temperature range and duration. Fig. 6 shows the two indices for the representative cities, where $I$ increased with the daily temperature range. The largest $I$ (102.4 °C·h) occurs in Dunhuang with 13.9 °C $T_R$. The smallest $I$ is 36.2 °C·h in Wuhan where $T_R$ is 5.7 °C. In Xi'an and Beijing, the values of $I$ are 55.8 °C·h and 44.2 °C·h, respectively, which are relatively low. The average $I$ ($I_{ave}$) for the outdoor air temperature in the representative cities (except for Wuhan) is 74.2 °C·h. The accumulated difference ($E$) values based on the outdoor air temperature and phase change temperature are shown in Fig. 6 (b). The largest $E$ (162 °C·h) is obtained in Turpan. However, the $E$ values in most representative cities are less than 0 °C·h, thereby indicating the potential requirements for passive cooling at night. When $E$ is below 0 °C·h, it is beneficial for the solidification of PCM to release the stored heat. The lowest $E$ (−202.6 °C·h) occurs in Xining. However, the phase change process could not proceed because the outdoor air temperature is below 26 °C.

This analysis of the climate characteristic indices ($T_R$, $T_{ave}$, $I$, and $E$) in the representative cities demonstrated that $T_R$ and $I$ are related to the potential application of PCM envelope. The thermal storage effect of PCM envelope is determined by the maximum/minimum temperature and $E$. Experiments are then conducted under representative climate conditions to investigate the relationships between the climatic

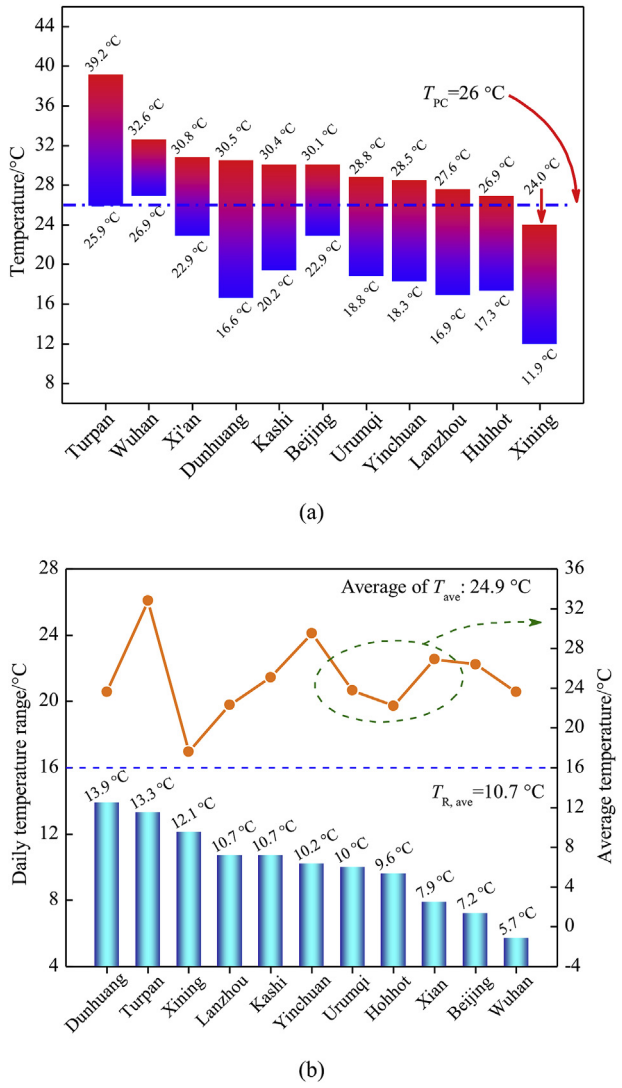


**Fig. 5.** Temperature range and average temperature in representative cities: (a) $T_{max}$ and $T_{min}$; (b) $T_R$ and $T_{ave}$.

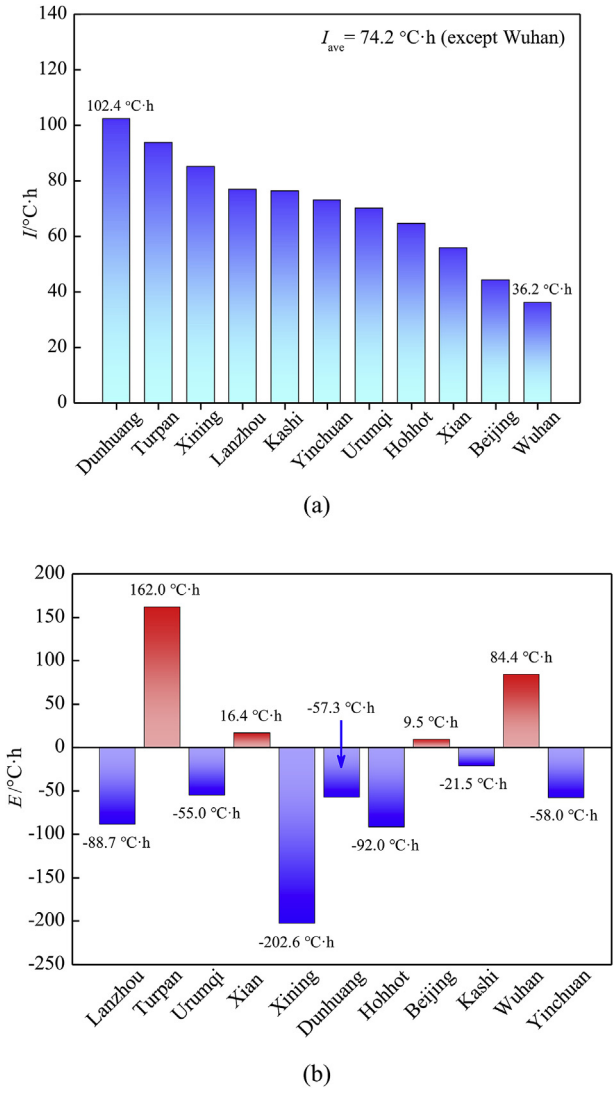


**Fig. 6.** Temperature characteristic indexes in representative cities: (a) *I*; (b) *E*.

characteristics and thermal performance of the PCM wallboard.

## 4. Results and discussion

### 4.1. Verification of experimentally controlled temperature

The accuracy of the controlled temperature curve is first verified by setting temperature curve. The controlled temperature and setting temperature curves are illustrated in Fig. 7. The controlled temperature is highly consistent with the temperature settings. The differences between the two temperature curves are shown in Fig. 8, which demonstrates that there are slight differences between air temperatures measured in the climate chamber and the set values. The average temperature difference is 0.64 °C. The differences are less than 1 °C in most of the experimental conditions. The maximum difference occurs in the conditions for Yinchuan condition (3.17 °C). However, the maximum difference only occurs for a short period in the experiment and it has no significant effect on the overall temperature curve. Therefore, the climate chamber performed well at simulating the typical climate conditions.

### 4.2. Temperature and heat flux of PCM wallboard under different climate conditions

A PCM wallboard can absorb and release latent heat only within a specific temperature range, and thus the thermal performance differs under various climate conditions. The temperature and heat flux are analyzed in order to investigate the thermal storage performance of the PCM wallboard under different climate conditions. The surface temperatures under the conditions in Turpan, Xining, Dunhuang, and Urumqi are illustrated in Fig. 9 as examples to show the differences in the thermal performance of the PCM wallboard. In Fig. 9, $T_{ex, air}$ is the outdoor air temperature of the test cell; $T_{in, air}$ is the indoor air temperature of the test cell; $T_{ex, sur}$ is the exterior surface temperature of the PCM wallboard; $T_{in, sur}$ is the interior surface temperature of the PCM wallboard. The temperature attenuation ratios for the PCM wallboard are up to 86.3% and 88.7% in the conditions for Dunhuang and Urumqi, respectively. However, the outdoor air temperature in Turpan is excessively high and it could not support the solidification and melting cycle in the PCM wallboard. In addition, the outdoor air temperature is quite low in Xining (24.8 °C), so the latent heat of the PCM could not be stored and released. Thus, the thermal storage effect of the PCM wallboard under the conditions in Xining condition is considerably inferior compared with those in Dunhuang and Urumqi. The temperature attenuation ratio under the conditions in Turpan is 70.1%, but only

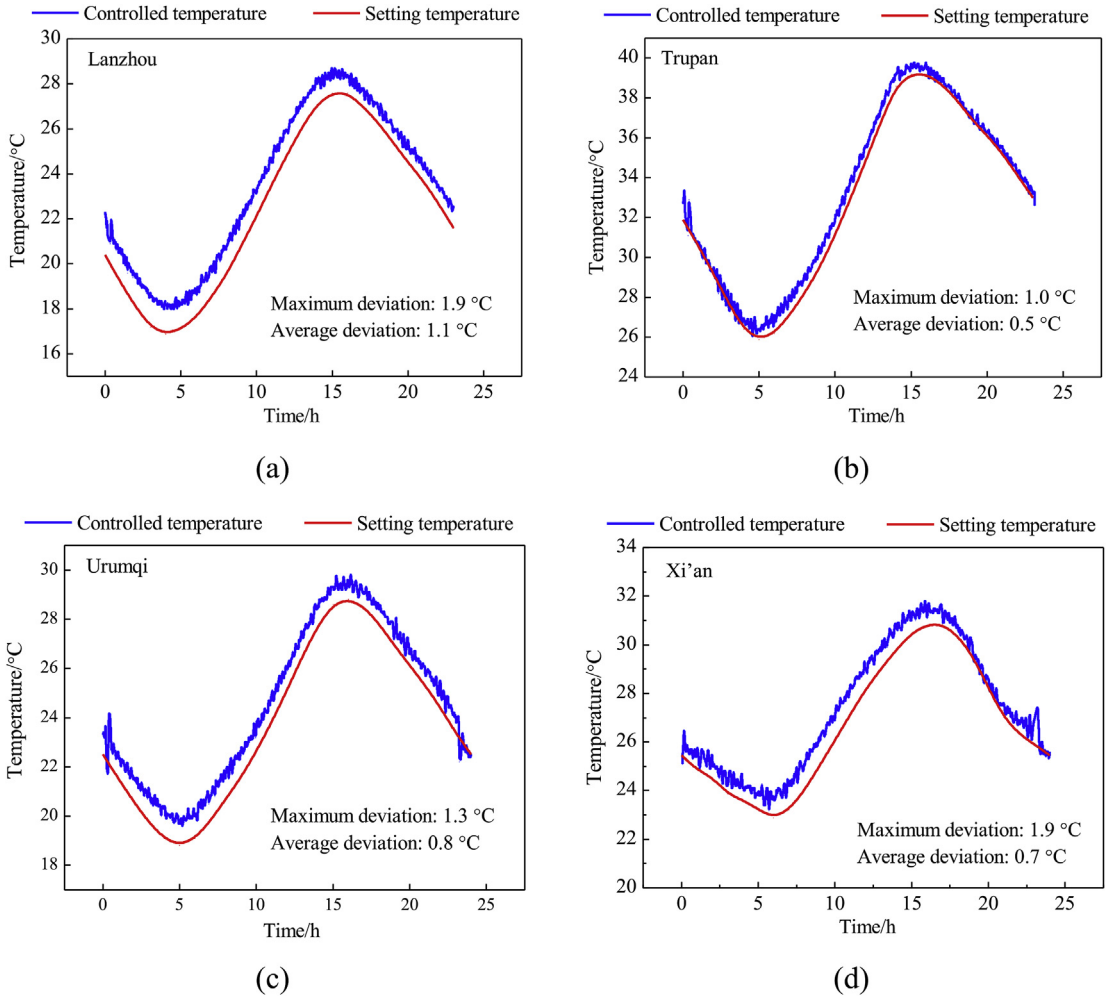


**Fig. 7.** Temperature curves of setting temperature and controlled temperature in different climate conditions: (a) Lanzhou; (b) Turpan; (c) Urumqi; (d) Xi'an.

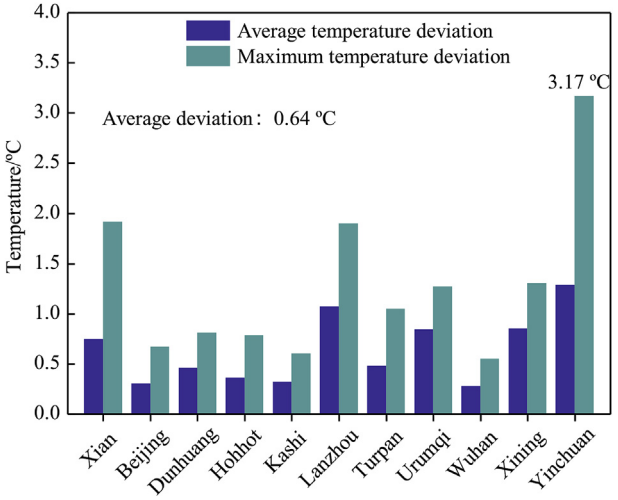


**Fig. 8.** Statistics of deviation between the setting temperature and experimental temperature.

53.78% under the conditions in Xining. The $T_R$ values are 7.9 °C and 10.0 °C in Xi'an and Urumqi, respectively. The temperature attenuation ratios under the conditions in these two cities are 86.5% and 88.7%, and thus they differ little in terms of the thermal storage effect. Therefore, the daily temperature range has only a slight effect on the thermal storage performance of the PCM wallboard. The PCM wallboard could stabilize the indoor air temperature under suitable temperatures but it cannot deliver excellent thermal storage performance if the outdoor air temperature is outside the range of the phase change temperature.

The temperature and heat flux curves obtained for the PCM wallboard under the climate conditions in Xi'an and Beijing are illustrated in Fig. 10. The temperature distribution of the PCM wallboard and test cell is shown in the upper portion of Fig. 10, where $T_{ex,\ air}$ is the outdoor air temperature of the test cell; $T_{in,\ air}$ is the indoor air temperature of the test cell; $T_{ex,\ sur}$ is the exterior surface temperature of the PCM wallboard; $T_{in,\ sur}$ is the interior surface temperature of the PCM wallboard. The heat flux distribution of the PCM wallboard surfaces is shown in the lower portion of Fig. 10, where $q_{ex,\ sur}$ is the heat flux on the exterior surface of the PCM wallboard; $q_{in,\ sur}$ is the heat flux on the interior surface of the PCM wallboard. The temperature attenuation ratios for the PCM wallboard are 86.5% and 80.5%, respectively, which represent the thermal performance during the phase change process. Fig. 10 (a) shows that, $T_R$ is 8.1 °C under the conditions in Xi'an, and the indoor air temperature amplitude in the test cells is only 2.4 °C. The maximum air temperature decreases from 32.3 °C to 26.9 °C, because of the improved of thermal storage performance. Fig. 10 (b) shows that under the conditions in Beijing, the maximum temperature decreases from 30.5 °C to 27.3 °C.

The heat flux changes with the surface temperature. The maximum temperature difference and the maximum heat flux occur at the same time. Due to the lack of thermal storage capacity in the insulation material, the change in the indoor air temperature is faster than that in

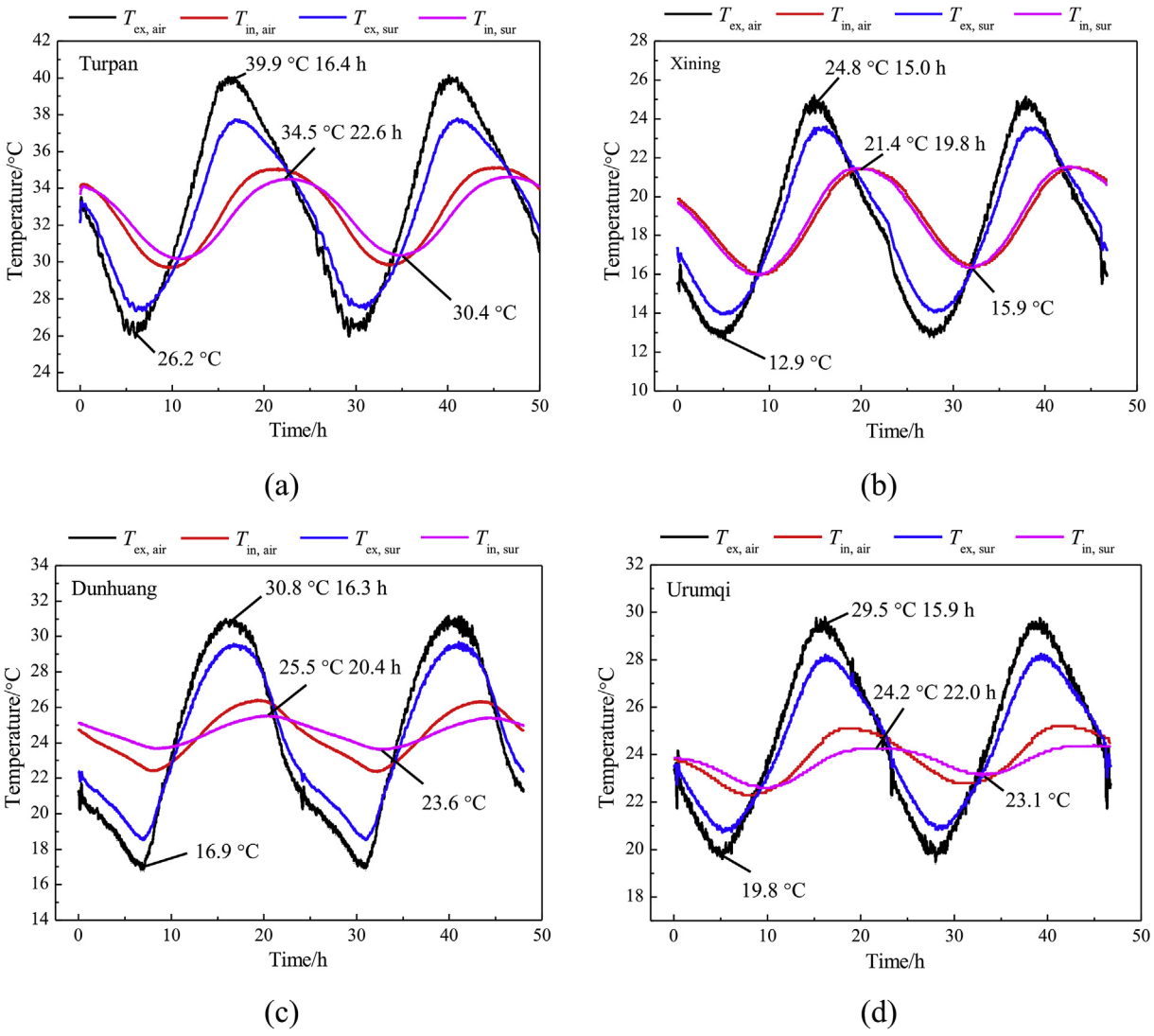


**Fig. 9.** PCM wallboard surface temperature in different climate conditions: (a) Turpan; (b) Xining; (c) Dunhuang; (d) Urumqi.

the interior surface temperature of the PCM wallboard. Therefore, there is a large time delay between the peak heat flux on the exterior and interior surfaces. Under the climate conditions in Xi'an and Beijing, the lag times for the heat flux is 12.2 h and 12.8 h, respectively. The largest difference in the indoor air and interior surface temperatures occurred under the conditions in Xi'an with 1.1 °C, where the peak heat flux on the interior surface is $-7.3\ W{\cdot}m^{-2}$. The heat flux curves showed that at high temperatures, the PCM wallboard absorbs the heat from the outdoor and indoor thermal environments simultaneously, but releases the heat with low air temperatures. Therefore, the PCM wallboard could reduce the indoor air temperature, but also delay the time until the response to hot outdoor air.

The thermal storage by the PCM wallboard is obtained from the heat flux curves. As shown in Fig. 10 (a), when the heat flux on the exterior surface is higher than $0\ W{\cdot}m^{-2}$, the wallboard absorbs the heat input from the outdoor environment. When the heat flux on the interior surface is less than $0\ W{\cdot}m^{-2}$, the wallboard absorbs heat from the indoor environment. Therefore, under the conditions in Xi'an, the heat absorption process by the wallboard exterior surface is from 9.3 h to 20.8 h (in a period), whereas the heat absorption process by the interior surface is from 0 h to 2.6 h and 11.1 h–24.0 h. At the time when the highest outdoor temperature occurred, the exterior/interior surfaces of the PCM wallboard undergo heat absorption, thereby effectively avoiding large fluctuations in the indoor air temperature. The thermal storage capacity of the PCM wallboard is calculated based on the area enclosed by the heat flux curves, which can be expresses as follows:

$$Q = \int_{t_1}^{t_2} q dt \tag{5}$$

where $Q$ is the thermal storage capacity; $q$ is the heat flux. Therefore, the thermal storage capacity of the PCM wallboard is obtained under the local climate conditions. Fig. 10 (a) shows that during a period of 24 h, the heat absorbed by the exterior surface is 1357.0 kJ and that absorbed by the interior surface is 2727.2 kJ. Thus, the heat absorbed by the PCM wallboard came mainly from the indoor environment. Therefore, during a period when the temperature changes, the PCM wallboard could absorb/release approximately 4084.2 kJ heat. The stored heat is equivalent to the heat absorbed by a clay brick wall with the same size and a thickness of 240 mm under a temperature increase of 12 °C. However, the temperature fluctuation in the PCM wallboard is only 0.7 °C on the interior surface and 7.1 °C on the exterior surface.

### *4.3. Relationship between the thermal performance of the PCM wallboard and climate characteristics*

The relationship between the phase change temperature and the outdoor air temperature is the most important factor that determine thermal storage performance of the PCM wallboard. As described in the

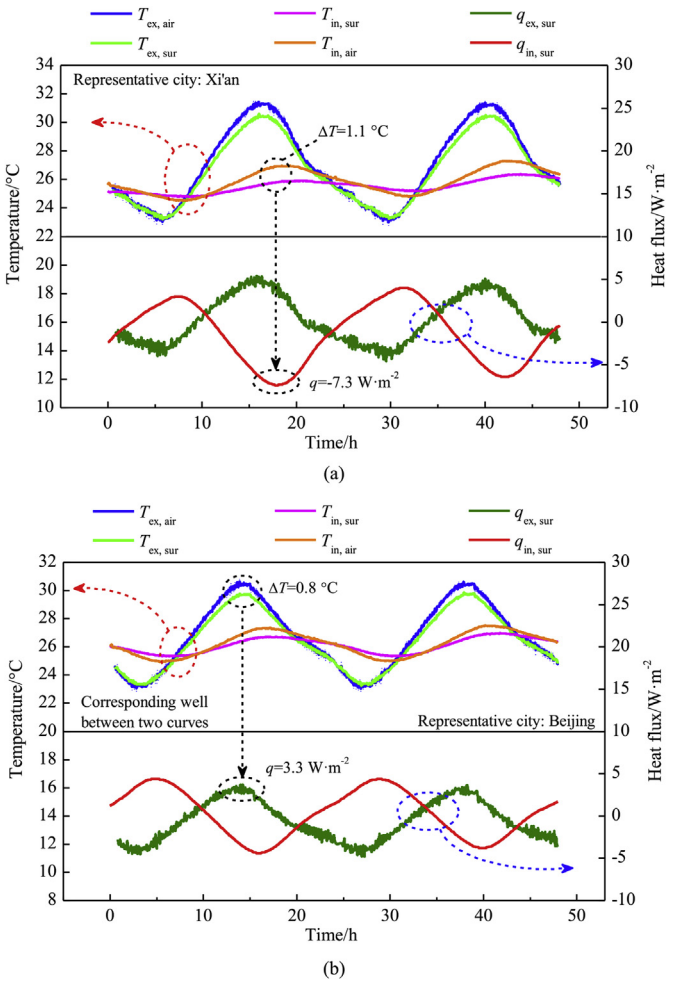


**Fig. 10.** Temperature and heat flux distribution of PCM wallboard: (a) Xi'an; (b) Beijing.

previous section, the dynamic thermal characteristics of the PCM wallboard are obtain by analyzing the temperature and heat flux. The climate characteristic indices ($I$ and $E$) are used to evaluate the relationship between the thermal storage performance of the PCM wallboard and the local climate characteristics. The $I$ values for the outdoor air and interior surface are shown in Fig. 11, which illustrates the attenuation of the temperature over time due to the cumulative effect. Remarkable thermal storage performance is determined for most of the representative cities. The attenuation ratios in terms of the degree hours of interior surface temperature are determined as higher than 75%. In particular, the attenuation ratios under the conditions on Xi'an and Kashi are over 88%.

By contrast, under the climate conditions in Turpan and Xining, the attenuation ratios are significantly lower those in the other representative cities (60.2% and 36.8%, respectively). In the reference city Wuhan, the attenuation ratio is 58.4%. However, due to the subtropical monsoon climate in Wuhan and the low daily temperature range, it is unnecessary to improve the thermal storage performance of the building envelope in this climate condition.

The parameters for different climate conditions and the thermal performance of the PCM wallboard are listed in Table 3. The parameters comprise the average outdoor air temperature ($T_{out,\ ave}$), accumulated outdoor air temperature ($I_{out,\ air}$), accumulated difference index ($E$), daily temperature range ($T_R$), temperature range of the PCM wallboard interior surface ($\Delta T$), temperature attenuation ratio ($P$), and temperature accumulative value for the PCM wallboard interior surface ($I_{in,\ sur}$). The characteristics of the outdoor air temperature and PCM envelope are represented by the index $E$. The thermal storage effect of the PCM envelope is evaluated using $P$. Therefore, nonlinear regression analysis is conducted to determine the relationship between the climate characteristics and the thermal performance of the PCM envelope. Fig. 12 shows the regression curve and equation. The experimental results are analyzed for the 10 representative climate conditions. A quadratic function is obtained between $P$ and $E$. In particular, the optimal thermal performance ($P_{max}$ = 88.4%) of the PCM wallboard is determined when $E$ is 3.2 °C·h. In most of the representative climate conditions, $E$ ranged from −100 °C·h to 50 °C·h. These results indicate that the utilization of PCM wallboard can improve the thermal performance of buildings in Northern and Western China. In practical applications, the thermal storage effect of the PCM wallboard can be estimated for specific climate conditions, where the temperature attenuation ratio can be calculated based on the typical meteorological year and the phase change temperature.

The accumulated difference index $E$ is proposed to quantitatively describe the local climate characteristics. The input parameter of $E$ is based on different conditions. In the present work, as the key parameter of the local climate characteristics, the dry-bulb temperature is adopted as the input parameter to calculate the accumulated difference index $E$. Therefore, the dry-bulb temperature of the representative cities is adopted in the experiments as the outdoor air temperature conditions. Based on the experimental results, the relationship between $E$ and the thermal storage effect of the PCM wallboard is obtained by nonlinear regression analysis.

However, when considering the integrated effects of solar radiation and outdoor air temperature in actual climate conditions, the concept of sol-air temperature ($T_{sa}$) can be adopted as the input parameters of the accumulated difference index $E$. In this case, the accumulated difference index $E$ can quantitatively describe the integrated effects of outdoor air temperature and solar radiation. Due to the input parameter is the sol-air temperature $T_{sa}$, the accumulated difference index $E$ can be expressed as:

$$E = \int_0^{24} (T_{sa} - T_{PC})dt \tag{6}$$

The sol-air temperature $T_{sa}$ can be defined as [39]:

$$T_{sa} = T_e + R(\alpha I_T - \varepsilon I_L) \tag{7}$$

where $T_e$ is the outdoor air temperature; $R$ is the thermal resistance of the external surface/air interface; $\alpha$ is the absorptivity for solar radiation; $\varepsilon$ is the emissivity for infrared radiation of the considered wall; $I_T$ is the intensity of direct plus diffuse solar radiation on the outer surface of the wall; $I_L$ is the intensity of long-wave radiation from a thermally black body at outdoor air temperature. When considering the integrated effects of solar radiation and outdoor air temperature, Eq. (6)

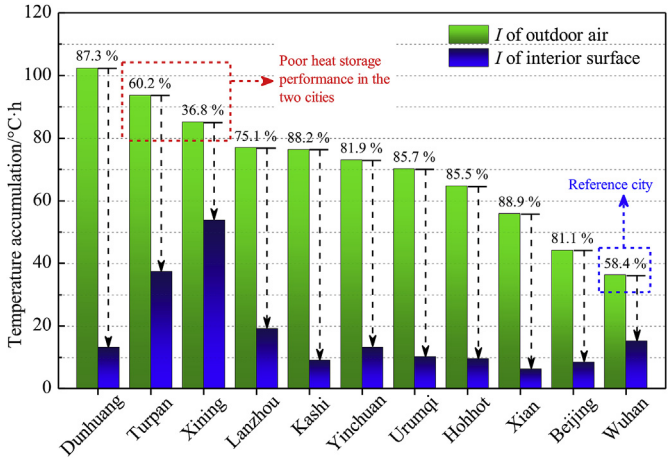


**Fig. 11.** Statistics of $I$ in representative cities.

**Table 3**
Parameters statistics of climate characteristics and thermal performance of PCM wallboard.

| | $T_{out,\ ave}$/°C | $I_{out,\ air}$/°C·h | $E$/°C·h | $T_R$/°C | $\Delta T$/°C | $P$/% | $I_{in,\ sur}$/°C·h |
|---|---|---|---|---|---|---|---|
| Lanzhou | 22.3 | 76.9 | −88.7 | 10.7 | 2.4 | 77.6 | 19.1 |
| Turpan | 32.8 | 93.7 | 162.0 | 13.3 | 4.1 | 69.2 | 37.3 |
| Urumqi | 23.8 | 70.1 | −55.0 | 10.0 | 1.1 | 89.0 | 10.0 |
| Xi'an | 26.9 | 55.8 | 16.4 | 7.9 | 0.7 | 91.0 | 6.2 |
| Xining | 17.6 | 85.1 | −202.6 | 12.1 | 5.5 | 54.5 | 53.8 |
| Dunhuang | 23.6 | 102.4 | −57.3 | 13.9 | 1.9 | 86.3 | 13.0 |
| Hohhot | 22.2 | 64.6 | −92.0 | 9.6 | 1.2 | 87.2 | 9.4 |
| Beijing | 26.4 | 44.2 | 9.5 | 7.2 | 1.4 | 81.1 | 8.4 |
| Kashi | 25.1 | 76.4 | −21.5 | 10.7 | 1.0 | 90.7 | 9.0 |
| Yinchuan | 23.6 | 73.0 | −58.0 | 10.2 | 1.6 | 84.5 | 13.2 |
| Wuhan | 29.5 | 36.2 | 84.4 | 5.7 | 2.0 | 64.9 | 15.1 |

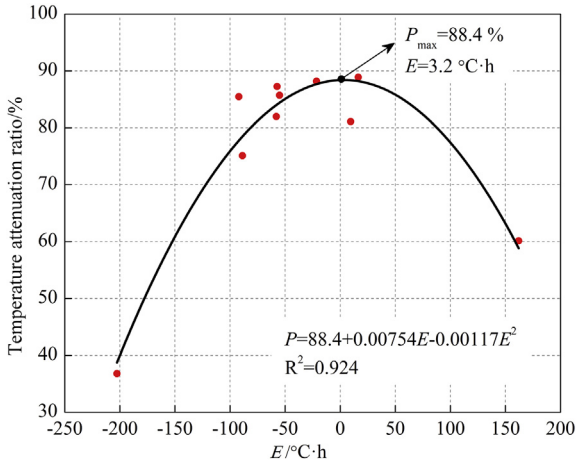


**Fig. 12.** Nonlinear regression analysis between $P$ and $E$.

can be adopted to calculate $E$ for estimating the thermal storage effect of the PCM wallboard by the nonlinear regression equation (see Fig. (12)).

## 5. Conclusions

In this study, reduced-scale experiments are conducted in an artificially controlled environment to investigate the thermal performance of PCM wallboard under the typical climate conditions in Northern and Western China. The dry bulb temperatures in 10 representative cities are first extracted based on typical meteorological year in order to obtain the experimentally controlled conditions. Two indices are developed to represent the climate characteristics. The thermal storage effect of the PCM wallboard is analyzed under the conditions in the representative cities based on the temperature and heat flux changes. Finally, the relationship between the climate characteristics and the thermal storage effect of the PCM wallboard is obtained by nonlinear regression analysis. The main findings obtained in this study are as follows.

(1) New evaluation indices are developed comprising the degree hours based on the average hourly temperature ($I$) and the accumulated difference between the outdoor air temperature and the phase change temperature over 24 h ($E$). The climate conditions can be quantitatively represented with these indices based on the effects of the temperature range and duration. The climate characteristics (as $T_R$, $T_{ave}$, $I$, and $E$) in 10 representative cities are considered in the present study. The climate conditions in Northern and Western China are typically characterized as dry hot climate. The average $T_R$ is 10.7 °C and $I$ is generally higher than 60 °C·h. $I$ and $E$ provide reference values for analyzing the requirements and assessing the possible use of PCM envelope under different climate conditions.
(2) The thermal storage performance of the PCM wallboard is determined under the typical climate conditions. According to the temperature and heat flux in the PCM wallboard under different climate conditions, the thermal storage effect of the PCM envelope is affected significantly by the outdoor air temperature. Under suitable climate conditions, the degree hours of the interior surface temperature are reduced by 88.9% and 88.2% for the representative conditions in Xi'an and Kashi, respectively. However, the reduction ratios are only 60.2% and 36.8% under the climate conditions with excessively high/low outdoor air temperatures during the phase change process, such as in Turpan and Xining.
(3) The relationship between the climate characteristics and thermal performance of the PCM wallboard is investigated by nonlinear regression analysis. A quadratic function is determined between the temperature attenuation ratio ($P$) and the accumulated temperature difference ($E$). The maximum temperature attenuation ratio is 88.4% when $E$ is 3.2 °C·h. This regression equation can provide a reference for assessing the suitability of applying PCM wallboard.

In the present study, quantitative indices were developed for analyzing climate characteristics. The results obtained could provide a reference for assessing the possible application of PCM envelope under different climate conditions.

## Acknowledgements

This work was supported by Natural Science Foundation of China (No. 51838011 and No. 51808429), Shaanxi Province Key Research and Development Plan (No. 2017ZDXM-SF-076), Natural Science Foundation of Shaanxi Province (No. 2017JQ5005) and Young Elite Scientists Sponsorship Program by CAST, YESS (No. 2018QNRC001).

## Appendix A. Supplementary data

Supplementary data to this article can be found online at https://doi.org/10.1016/j.buildenv.2019.106191.

## References

[1] S. Verbeke, A. Audenaert, Thermal inertia in buildings: a review of impacts across climate and building use, Renew. Sustain. Energy Rev. 82 (2018) 2300–2318.
[2] L. Yang, J.C. Lam, C.L. Tsang, Energy performance of building envelopes in different climate zones in China, Appl. Energy 85 (9) (2008) 800–817.
[3] Joseph C. Lam, Kevin K.W. Wan, C.L. Tsang, L. Yang, Building energy efficiency in different climates, Energy Convers. Manag. 49 (2008) 2354–2366.
[4] L. Navarro, A.D. Gracia, D. Niall, A. Castell, M. Browne, S.J. Mccormack, Thermal energy storage in building integrated thermal systems: a review. Part 2. Integration as passive system, Renew. Energy 85 (2) (2016) 1334–1356.
[5] X.R. Zhu, J.P. Liu, L. Yang, R.R. Hu, Energy performance of a new Yaodong dwelling, in the Loess Plateau of China, Energy Build. 70 (2014) 159–166.
[6] J.C. Lam, L. Yang, J.P. Liu, Development of passive design zones in China using bioclimatic approach, Energy Convers. Manag. 47 (6) (2006) 746–762.
[7] L. Zhang, A. Gustavsen, B.P. Jelle, L. Yang, T. Gao, Y. Wang, Thermal conductivity

of cement stabilized earth blocks, Constr. Build. Mater. 151 (2017) 504–511.
[8] Y. Liu, L. Yang, L.Q. Hou, S.Y. Li, J. Yang, Q.W. Wang, A porous building approach for modelling flow and heat transfer around and inside an isolated building on night ventilation and thermal mass, Energy 141 (2017) 1914–1927.
[9] L. Yang, Y.H. Qiao, Y. Liu, L.Q. Hou, M.Y. Wang, J.P. Liu, Review of phase change heat storage and night ventilation technology of buildings, Chin. Sci. Bull. 63 (2018) 629–640 (in Chinese).
[10] Y.P. Zhang, K.P. Lin, Q.L. Zhang, H.F. Di, Ideal thermophysical properties for free-cooling (or heating) buildings with constant thermal physical property material, Energy Build. 38 (10) (2006) 1164–1170.
[11] K.O. Lee, M.A. Medina, X.Q. Sun, X. Jin, Thermal performance of phase change materials (PCM)-enhanced cellulose insulation in passive solar residential building walls, Sol. Energy 163 (2018) 113–121.
[12] H.J. Akeiber, S.E. Hosseinia, H.M. Hussenc, M.A. Wahida, A.T. Mohammad, Thermal performance and economic evaluation of a newly developed phase change material for effective building encapsulation, Energy Convers. Manag. 150 (2017) 48–61.
[13] P. Schossig, H.M. Henning, S. Gschwander, T. Haussmann, Micro-encapsulated phase-change materials integrated into construction materials, Sol. Energy Mater. Sol. Cell. 89 (2) (2005) 297–306.
[14] A. Mourid, M.E. Alami, Frédéric Kuznik, Experimental investigation on thermal behavior and reduction of energy consumption in a real scale building by using phase change materials on its envelope, Sustain. Cities Soc. 41 (2018) 35–43.
[15] R. Barzin, J.J. Chen, B.R. Young, M.M. Farid, Application of PCM energy storage in combination with night ventilation for space cooling, Appl. Energy 158 (2015) 412–421.
[16] H.S. Ling, C. Chen, Y. Guan, S. Wei, Z.G. Chen, N. Li, Active heat storage characteristics of active–passive triple wall with phase change material, Sol. Energy 110 (2014) 276–285.
[17] K.P. Lin, Y.P. Zhang, X. Xu, H.F. Di, R. Yang, P.H. Qin, Experimental study of underfloor electric heating system with shape-stabilized PCM plates, Energy Build. 37 (3) (2005) 215–220.
[18] H.B. Kim, M. Mae, Y. Choi, Application of shape-stabilized phase-change material sheets as thermal energy storage to reduce heating load in Japanese climate, Build. Environ. 125 (2017) 1–14.
[19] F. Kuznik, J. Virgone, Experimental investigation of wallboard containing phase change material: data for validation of numerical modeling, Energy Build. 41 (5) (2009) 561–570.
[20] J.C. Xie, W. Wang, P.F. Sang, J.P. Liu, Experimental and numerical study of thermal performance of the PCM wall with solar radiation, Constr. Build. Mater. 177 (2018) 443–456.
[21] M. Iten, S.L. Liu, A. Shukla, Experimental study on the thermal performance of air-PCM unit, Build. Environ. 105 (2016) 128–139.
[22] L. Navarro, A. Solé, M. Martín, C. Barreneche, L. Olivieri, J.A. Tenorio, L.F. Cabeza, Benchmarking of useful phase change materials for a building application, Energy Build. 182 (2019) 45–50.
[23] X. Jin, M.A. Medina, X.S. Zhang, On the importance of the location of PCMs in building walls for enhanced thermal performance, Appl. Energy 106 (11) (2013) 72–78.
[24] E. Solgi, Z. Hamedani, R. Fernando, B.M. Karib, H. Skates, A parametric study of phase change material behaviour when used with night ventilation in different climatic zones, Build. Environ. 147 (2019) 327–336.
[25] F. Kuznik, J. Virgone, J.J. Roux, Energetic efficiency of room wall containing PCM wallboard: a full-scale experimental investigation, Energy Build. 40 (2) (2008) 148–156.
[26] F. Kuznik, J. Virgone, Experimental assessment of a phase change material for wall building use, Appl. Energy 86 (10) (2009) 2038–2046.
[27] X.Q. Sun, M.A. Medina, K.O. Lee, X. Jin, Laboratory assessment of residential building walls containing pipe-encapsulated phase change materials for thermal management, Energy 163 (2018) 383–391.
[28] J.C. Xie, W. Wang, J.P. Liu, S. Pan, Thermal performance analysis of PCM components heat storage using mechanical ventilation: experimental results, Energy Build. 123 (2016) 169–178.
[29] C.Y. Liu, Y.Y. Wu, Y.J. Zhu, D. Li, L.Y. Ma, Experimental investigation of optical and thermal performance of a PCM-glazed unit for building applications, Energy Build. 158 (2018) 794–800.
[30] F. Guarino, A. Athienitis, M. Cellura, D. Bastien, PCM thermal storage design in buildings: experimental studies and applications to solaria in cold climates, Appl. Energy 185 (2017) 95–106.
[31] H.M. Chou, C.R. Chen, V.L. Nguyen, A new design of metal-sheet cool roof using PCM, Energy Build. 57 (2013) 42–50.
[32] L. Yang, Y.H. Qiao, Y. Liu, X.R. Zhang, C. Zhang, J.P. Liu, A kind of PCMs-based lightweight wallboards: artificial controlled condition experiments and thermal design method investigation, Build. Environ. 144 (2018) 194–207.
[33] L. Yang, Y. Liu, Y.H. Qiao, J. Liu, M.Y. Wang, Building envelope with phase change materials. Zero and Net Zero Energy, IntechOpen (2019).
[34] H.Y. Yan, L. Yang, W.X. Zheng, W.F. He, D.Y. Li, Analysis of behaviour patterns and thermal responses to a hot-arid climate in rural China, J. Therm. Biol. 59 (2016) 92–102.
[35] J.E. Fernández, Materials for aesthetic, energy-efficient, and self-diagnostic buildings, Science 315 (5820) (2007) 1807–1810.
[36] L. Erlbeck, P. Schreiner, F. Fasel, F.J. Methner, M. Rädle, Investigation of different materials for macroencapsulation of salt hydrate phase change materials for building purposes, Constr. Build. Mater. 180 (2018) 512–518.
[37] K.K.W. Wan, S.L. Wong, L. Yang, J.C. Lam, An analysis of the bioclimates in different climates and implications for the built environment in China, Build. Environ. 45 (2010) 1312–1318.
[38] F. Kuznik, D. David, K. Johannes, J.J. Roux, A review on phase change materials integrated in building walls, Renew. Sustain. Energy Rev. 15 (1) (2011) 379–391.
[39] P.W. O'Callaghan, S.D. Probert, Sol-air temperature, Appl. Energy 3 (4) (1977) 307–311.